

## Sigma-Pi Interactions in Non-conjugated Polyalkynes: A Photoelectron Spectroscopic Study

Dennis L. Lichtenberger,<sup>\*,a</sup> Lalitha Subramanian,<sup>a</sup> Uwe Bunz†<sup>b</sup> and K. Peter C. Vollhardt<sup>b</sup>

<sup>a</sup> Laboratory for Electron Spectroscopy and Surface Analysis, Department of Chemistry, University of Arizona, Tucson, Arizona 85721, USA

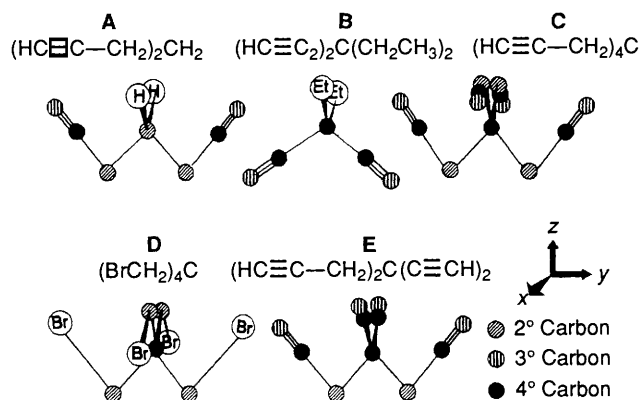
<sup>b</sup> Department of Chemistry, University of California, Berkeley, California 94720, USA

Through-space and through-bond interactions between  $\pi$ -orbitals in the molecules hepta-1,6-diyne (**A**), 3,3-diethylpenta-1,4-diyne (**B**), 4,4-diprop-2-ynylhepta-1,6-diyne (**C**), 2,2-di(bromomethyl)-1,3-dibromopropane (**D**) and 4,4-diethynylhepta-1,6-diyne (**E**) have been studied using gas-phase HeI photoelectron spectroscopy. The assignments of the photoelectron bands are discussed in relation to the results of extended Hückel calculations. Mixing of the  $\pi$  orbitals with the  $\sigma$  bond framework of the molecules is revealed by broadened band profiles in the  $\pi$  ionization region. Detailed examination of the first ionization of **A** suggests that one conformation is predominant under the conditions of the experiment. The terminal  $\pi$  orbitals are separated by too great a distance for through-space interaction, so the spread of the ionization band is entirely from through-bond interactions. The low-energy ionizations of **B** correspond to the in-plane and out-of-plane symmetric and antisymmetric combinations of the four terminal  $\pi$  orbitals, each of which has a different interaction with the C-H and C-C bonds of the central carbon atom. The spectra of **C** and **D** are very similar to each other, even though **C** has only alkyne substituents and **D** has only bromine substituents. The spectrum of **E** is a complicated mix of some of the features of **A** and some of the features of **B**. Extended Hückel calculations help clarify the number of orbitals in this region and the nature of the orbital interactions.

The study of non-bonding interactions in organic molecules containing two or more  $\pi$ -subunits, either conjugated or non-conjugated, is an important area of physical organic chemistry.<sup>1</sup> HeI photoelectron spectroscopy<sup>2</sup> has been the primary tool for experimentally quantifying these interactions. For example, photoelectron spectroscopic investigations of molecules with either acetylene functionalities or halogen substituents have given evidence of non-bonded interactions that occur by direct overlap between the  $\pi$  orbitals ('through-space' interaction) or that are mediated through intervening sigma bonds ('through-bond' interaction). Examples of specific systems that have been examined previously include simple molecules such as penta-1,4-diyne,<sup>3</sup> hexa-1,5-diyne,<sup>4</sup> hepta-1,6-diyne,<sup>5</sup> cyclooctadiyne<sup>6</sup> and related substrates<sup>7</sup> as well as bicyclo[2.2.2]octane and bicyclo[1.1.1]pentane derivatives of diynes and dihalides.<sup>8</sup> In most cases, the interaction of only two alkyne  $\pi$  moieties has been studied, partly because of the preparative inaccessibility of more highly decorated substrates.

We recently described the synthesis of the hitherto unknown tetraalkynes, namely, 4,4-dipropargylhepta-1,6-diyne<sup>†</sup> and 4,4-diethynylhepta-1,6-diyne.<sup>9</sup> These are interesting candidates for extension of the study of multiple bond interactions that can occur through-space and through-bond. Our aim is to study experimentally interactions in a few non-conjugated alkynes using photoelectron spectroscopy in an effort to understand the magnitude of through-bond and through-space interactions of  $\pi$  bonds.

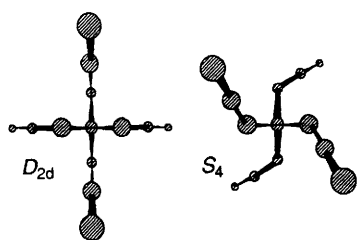
The systems included in this study are hepta-1,6-diyne (**A**), 3,3-diethylpenta-1,4-diyne (**B**), 4,4-dipropargylhepta-1,6-diyne (**C**), 2,2-di(bromomethyl)-1,3-dibromopropane (**D**) and 4,4-diethynylhepta-1,6-diyne (**E**) as shown below. The structures



shown are the most stable conformations as indicated by molecular mechanics calculations.<sup>10</sup> However, the barriers to rotation about certain bonds may be low and there may be more than one conformation present in the gas-phase. The favoured conformation for compound **C** (and **D**) reveals the two pairs of diagonally opposite propargyl (and  $\text{CH}_2\text{Br}$ ) arms forming a 'W' and an inverted 'W' about the central carbon atom. However, rotation of each propargyl (and  $\text{CH}_2\text{Br}$ ) arm must be considered. The 'W' conformation has a  $D_{2d}$  symmetry and this will be the geometry we will be mostly concerned with. Another favoured geometry looks like a 'swastika' when viewed down the rotation axis and has an  $S_4$  symmetry. The view down the  $z$ -axis is shown below. There are other conformations possible but they all have increasing numbers of interactions between C-X groups (X is  $\text{C}\equiv\text{C}$  or Br) at the ends of the chains.<sup>11</sup> Molecule **A** (hepta-1,6-diyne) can also exist in a 'W' or 'S' conformation while there is only one conformation possible for the substituted penta-1,4-diyne molecule **B** as far as the  $\pi$  orbitals are concerned. Molecule **E** can have different conformations in the gas-phase depending on the orientation of the

† Present address: Max-Planck-Institut f. Polymerchemie, W 6500 Mainz, Germany.

‡ Propargyl = prop-2-ynyl.

**Table 1** Extended Hückel parameters

Atom	Orbital	$H_{ii}/\text{eV}$	Slater exponent $\zeta$
C	2s	-21.4	1.625
	2p	-11.4	1.625
H	1s	-13.6	1.300
Br	4s	-22.07	2.588
	4p	-13.10	2.131

two propargyl arms. The presence of different conformations, leading to slightly different through-space interactions between the  $\pi$  bonds, could result in complicated photoelectron spectra with many overlapping bands.

### Experimental

**Data Collection.**—HeI gas-phase photoelectron spectra were recorded using an instrument that features a 36 cm hemispherical analyser with a 10 cm gap (McPherson). Spectra were collected by sweeping the voltage supplied to the spheres. Data collection methods are described elsewhere.<sup>12,13</sup> Molecules **A** and **B** are colourless liquids. Molecule **C** is a brownish white solid which sublimates at  $30 \pm 5^\circ\text{C}$ . Molecule **D** is a white crystalline solid which sublimates at  $60 \pm 5^\circ\text{C}$  at  $1 \times 10^{-6}$  Torr pressure. Molecule **E** is a colourless liquid. The solid samples were sublimed within the ionization chamber at low pressures while the liquid samples were leaked into the chamber through a needle valve. The count rate was high (600–1000 counts  $\text{s}^{-1}$ ) for all the samples except that for **B** (*ca.* 100 counts  $\text{s}^{-1}$ ). The total counts collected in the worst case (compound **B**) was about 2400 and in other cases was close to 9000. The argon  $2\text{P}_{3/2}$  ionization at 15.759 eV was used as an internal calibration lock of the energy scale. Using the position of the  $\text{CH}_3\text{I}$  iodine lone-pair ionization at 9.538 eV relative to Ar  $2\text{P}_{3/2}$  ionization, the kinetic energy scale was calibrated. The instrument resolution, measured using the Ar  $2\text{P}_{3/2}$  peak, was better than 30 meV during data collection. The data were intensity corrected for the experimentally determined analyser sensitivity *versus* electron kinetic energy. The close-up spectra are modelled analytically with asymmetric Gaussian peaks. The program is a modification of a previously published<sup>14</sup> one with the incorporation of constraints and boundary conditions used in the programs of Lichtenberger *et al.*<sup>15,16</sup> The bands are defined with the position, amplitude, halfwidth for the high binding energy side of the peak, and the halfwidth for the low binding energy side of the peak. The peak positions and halfwidths are reproducible to within about  $\pm 0.02$  eV ( $\approx 3\sigma$  level) when the peaks are not significantly overlapping. A minimum number of peaks was used to represent a band based solely on the visible contours of the band profile. The parameters describing an individual ionization peak are less certain when two or more peaks are close in energy and overlapping. Under such conditions the widths of the overlapping bands are constrained to each other. The confidence limits for the relative integrated peak areas are about 5%, with the primary source of uncertainty being the

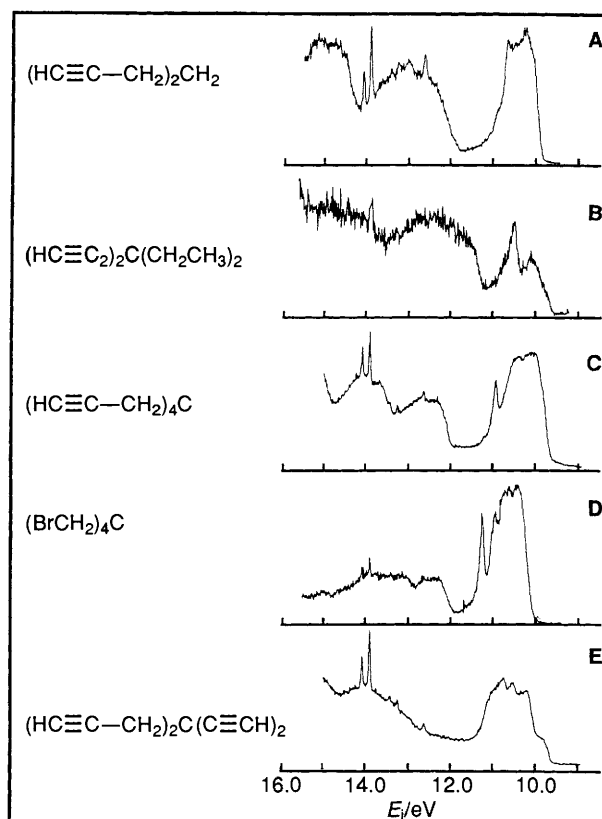


**Fig. 1** HeI photoelectron spectra of the full valence region for **A**, hepta-1,6-diyne; **B**, 3,3-diethylpenta-1,4-diyne; **C**, 4,4-dipropargylhepta-1,6-diyne; **D**, 2,2-di(bromomethyl)-1,3-dibromopropane and **E**, 4,4-diethynylhepta-1,6-diyne

determination of the baseline subtracted from the peak. More detailed discussion of modelling criteria are described in the literature.<sup>16</sup>

**Calculations.**—Extended Hückel calculations were used to assist the interpretation of the photoelectron spectra. The parameters<sup>17</sup> for the calculations are shown in Table 1. The program is an IBM PC version developed by Mealli and Proserpio.<sup>18</sup>

### Results and Discussion

Fig. 1 shows the full valence ionization region (8.5–16.0 eV) of the five non-conjugated  $\pi$ -systems. The region from 11.5–16.0 eV is a complex overlap of ionizations occurring from various C–C and C–H  $\sigma$  bonds. The region between 9.5–11.5 eV contains the information about interactions between  $\pi$  electrons. The alkyne-based  $\pi$  ionizations and, for **D**, the bromine  $\pi$  (lone pair) ionizations occur in this region. The photoelectron spectrum of the simple acetylene molecule<sup>2</sup> shows a well defined peak at 11.4 eV with vibrational fine structure. *n*-Propyl bromide also shows sharp peaks at 10.18 and 10.49 eV due to the bromine lone-pair ionizations.<sup>2</sup> Most conjugated alkynes have comparatively broad  $\pi$  ionizations<sup>4</sup> because of the mixing of the  $\pi$  orbitals. Similar broad-band profiles are present in these non-conjugated systems **A** to **E** indicating that there is a considerable amount of interaction of the  $\pi$  clouds either through space or through the intervening C–C and C–H  $\sigma$  bonds. It should be noted at this point that the onset of the C–C and C–H  $\sigma$  bond ionizations is generally within 1 eV or less of the  $\pi$  ionizations. The close energy proximity of these ionizations opens the possibility of orbital interactions.

Some other collective observations may be made. One striking feature is the similarity between the shapes of the first ionization bands in the spectra of **C** and **D** even though **C** is a tetrapropargyl molecule and **D** is a tetrabromo molecule. Both of these have a sharp peak on the high-energy side of the band. In the tetrabromo molecule the first broad feature is stabilized by about 0.5 eV compared with the tetrapropargyl molecule. It is also worth noting that the low energy band in hepta-1,6-diyne (**A**), which could be described as a dipropargyl molecule, is a little more than half the width of the first broad band in the tetrapropargyl molecule **C**. The spectrum of the substituted penta-1,4-diyne is different from the others as expected since this has fewer carbon atoms separating the triple bonded fragments. The last spectrum, molecule **E**, is complicated since it has some features of both **A** and **B**. The significance of these ionizations becomes more clear when the detailed features are examined individually.

**A Hepta-1,6-diyne.**—Fig. 2 shows the close-up spectrum of the region 9.5–11.5 eV for hepta-1,6-diyne. The variance at each data point is represented by the length of the vertical dash. The contour of the ionization band is represented analytically in terms of Gaussian peaks. This broad-band profile required a minimum of eight peaks to obtain a fairly good fit to the experimental spectrum. The peak parameters are listed in Table 2. The first three Gaussian peaks on the low-energy side are constrained to have the same shapes, and special significance should not be placed on the shape of any individual peak. The four peaks on the high-energy side represent vibrational fine structure on the tail of the broad ionization band. These peaks are also constrained to have the same shapes. The peaks are equally spaced within the certainty of the experiment and the spacing in this case is approximately  $900\text{ cm}^{-1}$ . This spacing is almost exactly one-half of the vibrational spacing that is observed in the photoelectron spectrum of the acetylene molecule. It follows that these peaks are the intermeshed progressions of two different ion states that are separated by about  $900\text{ cm}^{-1}$ . Looking at the higher intensity portion of the band, one can see four distinct ion states that are nearly evenly spread over about 0.6 eV in energy. In an earlier report<sup>5</sup> from a comparative study of the width of ionization bands for hepta-1,6-diyne, octa-1,7-diyne and nona-1,8-diyne it was concluded that the ionization band of hepta-1,6-diyne was most broad and this was attributed to the strength of interaction between the  $\pi$  orbitals. Their values for vertical ionizations match our peak positions to within  $\pm 0.03\text{ eV}$ . In order to gain a better understanding of this spectrum, it is helpful to consider the orbital interactions that lead to this splitting.

The experimentally observed splitting is generally a complicated interplay of both through-space and through-bond interactions. Through-space interaction between  $\pi$  systems is possible when they are forced into close proximity by, say, a constrained  $\sigma$  framework. As a first step, consider two acetylenic units in a plane. The linear combinations of the  $\pi$  orbitals will give rise to two symmetric and two antisymmetric combinations as shown below. The energy gap between the symmetric and antisymmetric orbitals of the out-of-plane combinations is

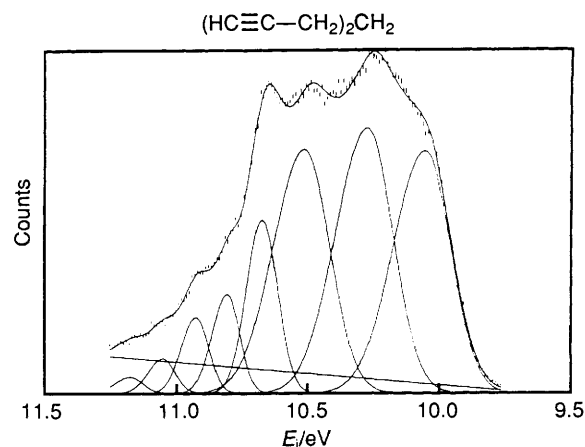
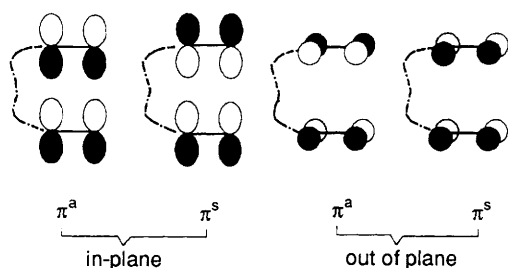


Fig. 2 Close-up photoelectron spectrum of hepta-1,6-diyne. The small vertical lines represent the variance at each experimental point.

Table 2 Peak parameters for hepta-1,6-diyne and 3,3-diethylpenta-1,4-diyne

Position (eV)	Width		Area
	High	Low	
<b>A Hepta-1,6-diyne</b>			
10.05	0.28	0.23	2.54
10.27	0.28	0.23	2.79
10.51	0.28	0.23	2.56
10.68	0.14	0.14	1.00
10.81	0.13	0.11	0.50
10.93	0.13	0.11	0.38
11.05	0.13	0.11	0.17
11.18	0.13	0.11	0.08
<b>B 3,3-diethylpenta-1,4-diyne</b>			
9.96	0.42	0.41	1.11
10.19	0.54	0.36	1.27
10.52	0.17	0.16	1.00
10.67	0.38	0.14	0.79

smaller than that between the in-plane combinations because of smaller through-space overlap for the out-of-plane orbitals. Furthermore, the splittings will be influenced by any interactions with the  $\sigma$ -framework that connects the two acetylenic units. To illustrate this, a semi-quantitative picture is shown in Fig. 3 based on extended Hückel calculations. Here the interaction of the in-plane  $\pi$  molecular orbitals with different numbers of carbon atoms separating them is shown. Calculations were carried out for penta-1,4-diyne, hexa-1,5-diyne and hepta-1,6-diyne. The geometry for penta-1,4-diyne has no significant degrees of freedom. For hepta-1,6-diyne, the two propargyl arms having the  $\pi$  orbitals are relatively free to rotate, but they prefer to remain in an 'open' conformation due to steric reasons. The geometry selected for the hexa-1,5-diyne is an intermediate between the 5-carbon and 7-carbon systems (**I** and **III**) for purposes of illustration, though this is not energetically the most favoured conformation. In Fig. 3, **I(a)**, **II(a)** and **III(a)** indicate the energy levels for two separate acetylene units maintained at the same geometry as the molecule shown except that the intervening  $\text{CH}_2$  groups have been removed. Thus the levels shown under (a) are due to through-space interactions alone. In **I(b)**, **II(b)** and **III(b)** both through-space and through-bond interactions are present. Consider the splitting of levels under (a) for all the three molecules. The shortest distance between the  $\text{C}\equiv\text{C}$  units in penta-1,4-diyne is  $2.377\text{ \AA}$ , in hexa-1,5-diyne it is  $2.514\text{ \AA}$  and in hepta-1,6-diyne it is  $4.899\text{ \AA}$ . Due

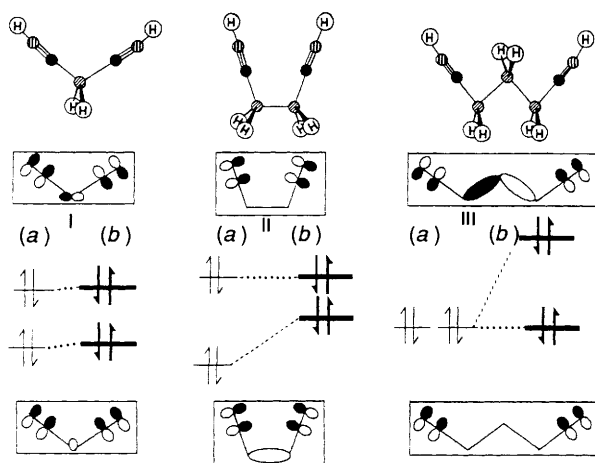


Fig. 3 In-plane orbitals of (a) two separate acetylene units split by through-space interactions and (b) two terminal alkyne units in the presence of through-bond and through-space interactions

to through-space interaction, there is a stabilization of the symmetric  $\pi^s$  orbital and a destabilization of the antisymmetric  $\pi^a$  orbital. The through-space interaction is largest for **II(a)** because the geometry used here forces a better overlap of orbitals through space. In **III(a)** the distance is too large and the symmetric and antisymmetric in-plane orbitals are essentially degenerate.

Since the symmetric and antisymmetric orbitals have different symmetries with respect to a vertical plane of symmetry between the two  $C\equiv C$  units, their interaction with a connecting  $\sigma$ -framework is also going to be different. In the penta-1,4-diyne, the methylene bridge has appropriate orbitals that destabilize both the symmetric and antisymmetric combinations very slightly as shown in **I(b)**. In the case of **II(b)**, there are two  $CH_2$  units separating the two  $\pi$  units. The symmetric orbital is destabilized to a large extent while there is no  $\sigma$  orbital appropriate for interaction with the antisymmetric combination, and this is not affected. In hepta-1,6-diyne, **III(b)**, the antisymmetric orbital is destabilized through interaction with the antisymmetric combination of the  $C-C$   $\sigma$  bond orbitals. There is also a symmetric combination of the  $C-C$   $\sigma$  bonding orbitals which, however, is much more stable and interacts very little with the  $\pi$  orbitals. In the hepta-1,6-diyne, the in-plane antisymmetric  $\pi$  orbital (destabilized by  $\sigma$  interaction) is calculated to be the HOMO. The second highest occupied molecular orbital is the out-of-plane antisymmetric combination of the  $\pi$  orbital. Below this, the calculation places the in-plane symmetric and out-of-plane symmetric orbitals close in energy. The splitting between the in-plane symmetric and antisymmetric combinations of  $\pi$  orbitals is 0.5 eV and that for the out-of-plane orbitals is 0.07 eV.

Moreover, it must be considered that more than one rotamer can be present in the gas phase. Fig. 4 shows a Walsh diagram for the conformational change from an 'S' to a 'W' based on extended Hückel calculations, which usually give a fairly good estimate of the rotational barrier for molecules such as these.<sup>19</sup> There is an activation barrier of about 8 kcal mol<sup>-1</sup> for interconversion between the 'W' conformation and the next most stable conformation, the 'S', in which one propargyl group has been rotated 180° around the central carbon atom. Through-space interactions are negligible and through-bond interactions change slightly with angle. There is not much change in the energies of the four relevant  $\pi$  orbitals, so that they would all appear in the same overlapping ionization envelope. The fact that four individual peaks can be distinguished on the top of the broad ionization band suggests

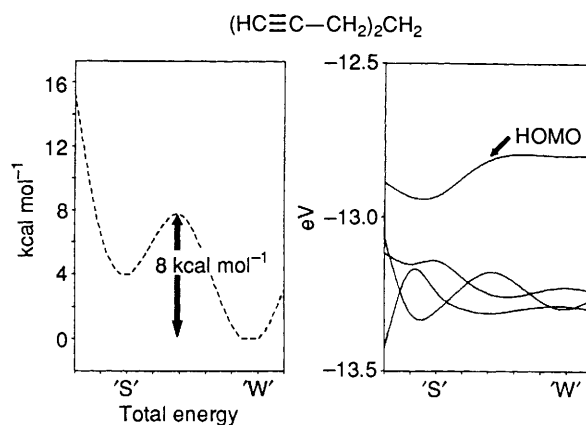


Fig. 4 Walsh diagram for rotation of hepta-1,6-diyne from 'S' to 'W' conformation

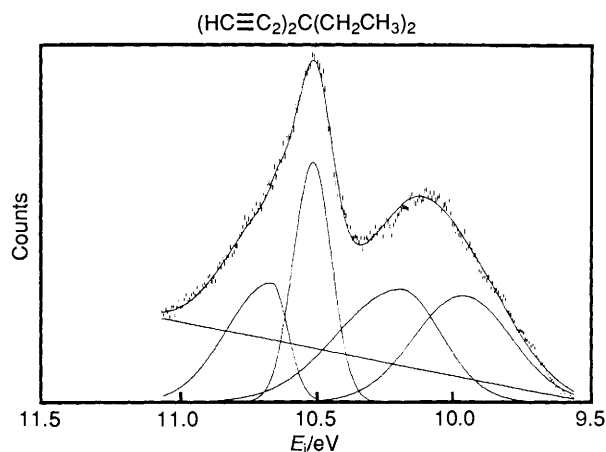


Fig. 5 HeI photoelectron spectrum of substituted penta-1,4-diyne

that a single conformation is predominant under the conditions of our experiment.

**B 3,3-Diethylpenta-1,4-diyne.**—Fig. 5 shows the low binding energy HeI photoelectron spectrum of the substituted penta-1,4-diyne. This system has only one possible conformation as far as the triple-bonded units are concerned. A spectrum of unsubstituted penta-1,4-diyne has been reported previously.<sup>3</sup> However, only the full valence region was reported and the spectrum shown is not very clear. The general shape appears similar to the spectrum reported here. Table 2 lists the analytical representation of the ionizations between 9.5 and 11.0 eV. The widths and contours of the ionization bands between 9.5 and 11 eV suggest the presence of four ionization states, as expected for the four combinations of  $\pi$  orbitals in this molecule. A minimum of four peaks are required for a reasonable representation of the ionization contours. The peak areas are approximately equal. Vibrational progressions are hinted at on the high binding energy sides of the bands but are not obvious in this spectrum.

Calculations (performed on the unsubstituted penta-1,4-diyne instead of the diethyl derivative) reveal the HOMO to be the in-plane antisymmetric  $\pi$ -orbital combination, just as in the case of hepta-1,6-diyne. Below this is the out-of-plane symmetric combination, followed by the out-of-plane antisymmetric combination and the in-plane symmetric combinations of the  $\pi$  orbitals. It is interesting that the order of the out-of-plane symmetric and antisymmetric combinations is reversed from the expectations of through-space interactions. The out-of-plane symmetric  $\pi$  orbital combination has 85% contribution from the  $\pi$  orbitals and the rest from the p orbital of the central carbon atom (antisymmetric combination of the  $C-H$   $\sigma$  bonds).

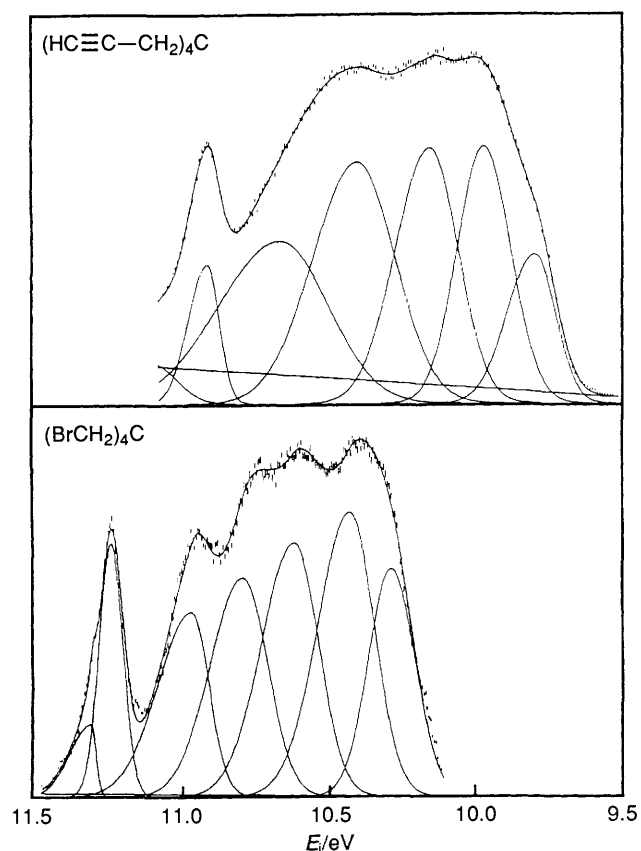


Fig. 6 HeI photoelectron spectra of 4,4-dipropargylhepta-1,6-diyne and 2,2-di(bromomethyl)-1,3-dibromopropane in the region 9.5–11.5 eV

Table 3 Peak parameters for 4,4-dipropargylhepta-1,6-diyne and 2,2-di(bromomethyl)-1,3-dibromopropane

Position (eV)	Width		Relative area
	High	Low	
<b>C 4,9-dipropargylhepta-1,6-diyne</b>			
9.79	0.22	0.16	1.00
9.97	0.21	0.21	1.92
10.15	0.28	0.22	2.25
10.40	0.36	0.30	2.82
10.66	0.48	0.39	2.50
10.91	0.15	0.10	0.61
<b>D 2,2-Di(bromomethyl)-1,3-dibromopropane</b>			
10.28	0.19	0.19	1.80
10.43	0.26	0.20	2.78
10.62	0.26	0.20	2.48
10.79	0.26	0.20	2.14
10.97	0.27	0.14	1.63
11.24	0.09	0.09	1.00

This through-bond interaction destabilizes the orbital ionization of the symmetric combination of the out-of-plane  $\pi$  orbitals due to the antibonding mixing with the p orbital of the central carbon. In contrast, the central carbon atom has no orbitals of the correct symmetry to interact with the out-of-plane antisymmetric combination, and this orbital thus has 100% contribution from the  $C\equiv C$   $\pi$  orbitals. This latter orbital gives a sharp ionization peak at 10.52 eV. The sharpness of the peak is consistent with the lack of mixing with the  $\sigma$  framework and less vibrational excitation with ionization. The position of the ionization is consistent with the  $\pi$  ionization of methyl acetylene which is at 10.37 eV.<sup>2</sup> This ionization might be

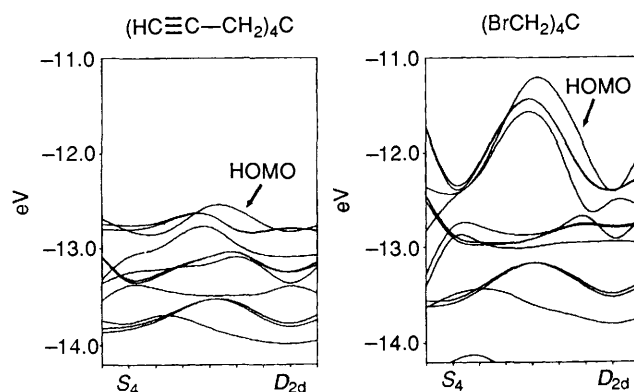
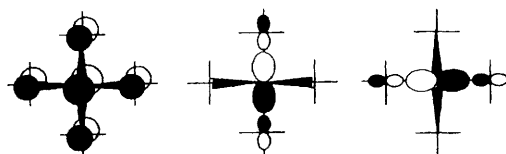


Fig. 7 Walsh diagram for 4,4-dipropargylhepta-1,6-diyne and 2,2-di(bromomethyl)-1,3-dibromopropane

expected to exhibit a vibrational progression in the  $C\equiv C$  stretch, but in this case the high binding energy side of the peak is partly obscured by another broad ionization band. This latter ionization is assigned to the symmetric, in-plane combination of the  $\pi$  orbitals.

**C 4,4-Dipropargylhepta-1,6-diyne and D 2,2-Di(bromomethyl)-1,3-dibromopropane.**—Fig. 6 shows the close-up HeI photoelectron spectra for the tetrapropargyl and tetrabromo molecules. Their spectra are similar except for a stabilization of the bands in the latter by about 0.5 eV. The peak parameters are listed in Table 3. Extended Hückel calculations place the first eleven levels fairly close in energy. This corresponds to 22 electrons in the first ionization band shown in Fig. 6. Eight  $\pi$ -based levels are expected from the four propargyl groups or the four bromine atoms. Three additional levels arise from the central carbon framework. Specifically, if one considers the neopentane skeleton which is present in these two systems, there is a triply degenerate ( $t_2$ ) level as shown below composed primarily of the  $p_x$ ,  $p_y$  and  $p_z$  orbitals of the carbon atoms (the central carbon atom and the surrounding  $CH_3$  groups). In neopentane, the onset of this ionization occurs at 10.9 eV.<sup>2</sup> In



the presence of the terminal Br or acetylene unit, we can envisage this set to stabilize slightly but it is likely that this set is still in the region 9.5–11.5 eV. Therefore, these three levels also contribute to the ionization in the near valence region and this results in eleven levels close together in energy in the  $\pi$  ionization region.

Klaeboe *et al.*<sup>20</sup> have studied the conformations of 2,2-di(bromomethyl)-1,3-dibromopropane. They report that in the crystalline state, there is only the  $D_{2d}$  conformer present. Our extended Hückel, MM2<sup>21</sup> and MOPAC/MNDO<sup>22</sup> (version 5.0) calculations on both hepta-1,6-diyne and the tetrapropargyl systems indicate the  $D_{2d}$  conformation is favoured, but the energy barrier to rotation from  $D_{2d}$  to  $S_4$  is fairly small (< 10 kcal mol<sup>-1</sup>). These calculations involved rotating one bond at a time. Fig. 7 shows the Walsh diagram for the tetrapropargyl and tetrabromo systems when all four bonds are rotated simultaneously. The energy variation of individual orbitals with rotation from an  $S_4$  to a  $D_{2d}$  conformation indicates that in the  $D_{2d}$  conformation the eleventh level is fairly well separated from the first ten levels. The observation of the sharp peak on the high

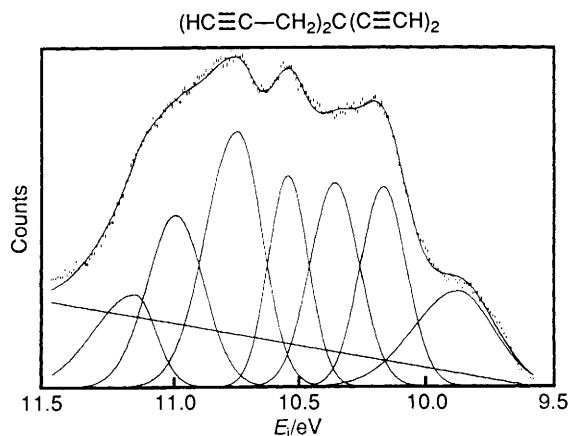
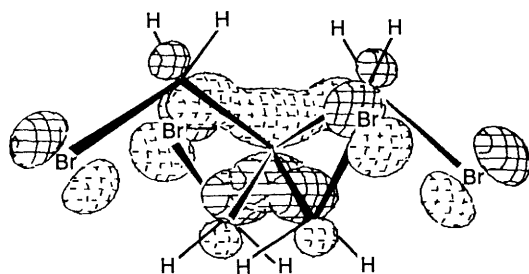


Fig. 8 HeI photoelectron spectrum for 4,4-diethynylhepta-1,6-diyne

Table 4 Peak parameters for 4,4-diethynylhepta-1,6-diyne (E)

Position (eV)	Width		Relative area
	High	Low	
9.87	0.42	0.33	1.00
10.16	0.21	0.21	1.23
10.36	0.23	0.23	1.34
10.54	0.19	0.19	1.13
10.74	0.30	0.23	1.95
10.99	0.26	0.26	1.29
11.15	0.37	0.19	0.74

energy side of the valence ionization band is evidence in support that the  $D_{2d}$  rotamer is present to an appreciable amount and not the  $S_4$  rotamer. This feature is seen for both of the molecules. A representation<sup>18</sup> of this orbital which gives rise to the sharp peak on the high energy side is shown below. The orbital for the tetrapropargyl molecule is very similar. The  $p_z$  orbital of the central carbon atom is bonding to the four  $\text{CH}_2$  units around it. The  $p$  orbitals on the Br atoms are almost non-bonding.



**E 4,4-Diethynylhepta-1,6-diyne.**—Fig. 8 shows the low ionization energy HeI photoelectron spectrum for this molecule. The parameters of the analytical representation of the ionization contour are listed in Table 4. Calculations show eight levels in this region. The  $t_2$  level of the neopentyl skeleton is absent here and therefore we get eight levels as expected in this region 9.5–11.5 eV. Since the peaks overlap to a large extent, no attempt is made to assign the individual peaks. A comparison between the spectrum of the tetrapropargyl molecule and this system reveals the onset of ionization to be almost the same in these two cases. The intensity of the lowest energy band seems to have decreased in E compared with C. This indicates that the first band may be due to ionization from the  $\pi$  system of the propargyl group rather than the ethynyl group. In E, there is a shoulder at approximately 10.5 eV which is close to the position of the out-

of-plane non-bonding  $\pi$  orbital which comes up as a sharp peak in the substituted penta-1,4-diyne. In general, the low valence ionization region of E appears as a combination of the ionizations of A and B.

### Discussion

A number of common features emerge from the study of this collection of terminal diyne and tetrayne molecules. All of these molecules show substantial coupling of the  $\pi$  orbitals that splits the  $\pi$ -based ionizations over a range from 0.6 eV to more than 1 eV. Through-space interactions between  $\pi$  orbitals can be substantial, but the terminal propargyl groups of these molecules are relatively free to rotate to favoured conformations, and the conformations with maximum through-space interaction are not favoured sterically. The spectra suggest that a single conformation is predominant in the gas phase in each case. The splitting of the  $\pi$ -based ionizations is sensitive to the mixing of these orbitals with the  $\sigma$  bonding framework of the molecule. Symmetry governs which combinations of C–C and C–H  $\sigma$  orbitals can interact with which combinations of the  $\pi$  orbitals, and the energy separation of the appropriate  $\sigma$  orbitals from the  $\pi$  orbitals has a strong effect on the extent of mixing and the shift of the  $\pi$ -based ionizations. In the simple substituted penta-1,4-diyne system there is a narrow peak at 10.52 eV which is due to a pure  $\pi$  ionization without  $\sigma$  character. It corresponds to the antisymmetric combination of the out-of-plane  $\pi$  orbitals, for which there are no orbitals on the central carbon atom of the correct symmetry. At lower ionization energy is the corresponding symmetric  $\pi$  combination, which is destabilized by interaction with the appropriate combination of the C–H  $\sigma$  bonds on the central carbon. In the case of hepta-1,6-diyne, the terminal alkynes are sufficiently separated that the through-space interaction is negligible, but the  $\pi$ -based ionizations are still substantially split. In this case the splitting is clearly caused by interactions with the  $\sigma$  framework, and the strongest interactions are with antisymmetric combinations of the  $\sigma$  bonds, which are closest in energy to the  $\pi$  bonds. For the tetrapropargyl and tetrabromo molecules, the observation of a relatively intense, sharp ionization in each case is a strong indication of the predominance of a single conformation for these molecules in the gas phase. Calculations indicate that this is the  $D_{2d}$  conformation, consistent with the structure found in the crystal. Again, the energy spread of the ionizations indicates interaction with the  $\sigma$  framework and in this case a set of three  $\sigma$ -based orbitals is in the same energy region. The 4,4-diethynylhepta-1,6-diyne gives rise to a complex spectrum of overlapping bands with some ionizations similar to those seen in the tetrapropargyl molecule and some similar to those seen in penta-1,4-diyne. Thus the coupling of the  $\pi$  orbitals with the  $\sigma$  framework remains similar, and there is little additional direct coupling of the  $\pi$  orbitals through space.

### Acknowledgements

L. S. acknowledges the help of Abby Parrill for the MM2 and MOPAC/MNDO calculations. D. L. L. and L. S. acknowledge the Department of Energy (Division of Chemical Sciences, Office of Basic Energy Sciences, Office of Energy Research; Contract No. DE-FG02-86ER13501) and the National Science Foundation (CHE-9300841) for financial support. U. B. thanks the DFG for a postdoctoral fellowship (1991–1992). K. P. C. V. acknowledges the National Science Foundation (NSF 92-02152) for financial support.

### References

- (a) R. Gleiter, *Angew. Chem.*, 1992, **104**, 29; *Angew. Chem., Int. Ed. Engl.*, 1992, **31**, 27; (b) R. Gleiter and W. Schäfer, *Acc. Chem. Res.*,

- 1990, **23**, 369; (c) R. Gleiter, *Pure Appl. Chem.*, 1987, **59**, 1585; (d) L. T. Scott, *Pure Appl. Chem.*, 1986, **58**, 105; (e) H. D. Martin and B. Mayer, *Angew. Chem.*, 1983, **95**, 281; *Angew. Chem., Int. Ed. Engl.*, 1983, **22**, 283; (f) M. N. Paddon-Row, *Acc. Chem. Res.*, 1982, **15**, 245; (g) R. Gleiter, *Angew. Chem.*, 1974, **86**, 770; *Angew. Chem., Int. Ed. Engl.*, 1974, **13**, 698; (h) R. Hoffmann, *Acc. Chem. Res.*, 1971, **4**, 1; (i) M. N. Paddon-Row and K. D. Jordan, *J. Am. Chem. Soc.*, 1993, **115**, 2952; (j) R. Gleiter, R. Merger and H. Irngartinger, *J. Am. Chem. Soc.*, 1992, **114**, 8927.
- 2 D. W. Turner, C. Baker and R. C. Brundle, *Molecular Photoelectron Spectroscopy*, Wiley-Interscience, London, 1950; K. Kimura, S. Katsumata, Y. Achiba, T. Yamazaki and S. Iwata, *Handbook of HeI Photoelectron Spectra of Fundamental Organic Molecules*, Japan Scientific Society Press, Tokyo, 1981.
- 3 F. Brogli, E. Heilbronner, J. Wirz, E. Kloster-Jensen, R. G. Bergman, K. P. C. Vollhardt and A. J. Ashe III, *Helv. Chim. Acta*, 1975, **58**, 2620.
- 4 P. Bischof, R. Gleiter, H. Hopf and F. T. Lenich, *J. Am. Chem. Soc.*, 1975, **97**, 5467.
- 5 E. Nagy-Felsobuki, J. B. Peel and G. D. Willett, *Chem. Phys. Lett.*, 1979, **68**, 523.
- 6 G. Bieri, E. Heilbronner, E. Kloster-Jensen, A. Schmelzer and J. Wirz, *Helv. Chim. Acta*, 1974, **57**, 1265.
- 7 R. Gleiter, D. Kratz, W. Schäfer and V. Schlmann, *J. Am. Chem. Soc.*, 1991, **113**, 9258.
- 8 (a) E. Honegger, E. Heilbronner, N. Hess and H. D. Martin, *Chem. Ber.*, 1987, **120**, 187 and references therein; (b) R. Gleiter, K.-H. Pfeifer, G. Szeismies and U. Bunz, *Angew. Chem.*, 1990, **102**, 418; *Angew. Chem., Int. Ed. Engl.*, 1990, **29**, 413.
- 9 U. Bunz, K. P. C. Vollhardt and J. S. Ho, *Angew. Chem.*, 1992, **104**, 1645; *Angew. Chem., Int. Ed. Engl.*, 1992, **31**, 1648.
- 10 We used AM1 and MM2 calculations to arrive at the most stable conformation.
- 11 R. Stolvik and P. Bakken, *J. Mol. Struct.*, 1986, **140**, 193.
- 12 G. E. Kellogg, *Diss. Abstr. Intl.*, 1986, **46**, 3838.
- 13 M. E. Jatcko, *Diss. Abstr. Intl. B*, 1990, **51**(1), 200.
- 14 G. V. R. Chandramouli, S. Lalitha and P. T. Manoharan, *Comput. Chem.*, 1990, **14**, 257.
- 15 D. L. Lichtenberger and R. F. Fenske, *J. Am. Chem. Soc.*, 1976, **98**, 50.
- 16 D. L. Lichtenberger and A. S. Copenhaver, *J. Electron Spectrosc. Relat. Phenom.*, 1990, **50**, 335.
- 17 (a) R. Hoffmann, *J. Chem. Phys.*, 1963, **39**, 1397; (b) S. Alvarez, F. Mota and J. Novoa, *J. Am. Chem. Soc.*, 1987, **109**, 6586.
- 18 C. Mealli and D. M. Proserpio, *J. Chem. Educ.*, 1990, **67**, 399.
- 19 J. P. Lowe, *J. Am. Chem. Soc.*, 1974, **96**, 3759.
- 20 P. Klaboe, B. Klewe, K. Martinsen, C. J. Nielson, D. L. Powell and D. J. Stubbles, *J. Mol. Struct.*, 1986, **140**, 1.
- 21 U. Burkert and N. L. Allinger, *Molecular Mechanics*, American Chemical Society, Washington DC, 1982.
- 22 J. J. P. Stewart, *J. Comput. Aided Molecular Design*, 1990, **4**, 1.

Paper 3/06990G

Received 23rd November 1993

Accepted 23rd February 1994